Cell fate specification based on tristability in the inner cell mass of mouse blastocysts

Laurane De Mot, Didier Gonze, Sylvain Bessonnard, Claire Chazaud, Albert Goldbeter, Geneviève Dupont

Supporting information

Model description

1. Gene regulatory network : one cell model

Nanog and Gata6 are required for the proper specification of Epi and PrE cells, respectively, and thus constitute the core of the GRN described in the model. These transcription factors inhibit each other and activate their own expression (1-8). Even though it was recently shown that Nanog can repress its own expression in ES cells (9), this autorepression does not seem to occur during preimplantation embryogenesis stages (8) and it is thus not included in the model.

Besides the interactions between Gata6 and Nanog, the model incorporates the role of the Fgf/Erk signaling pathway, which is activated through the binding of Fgf4 to the receptor FGFR2. Experiments on Nanog$^{-/-}$ and Gata6$^{-/-}$ embryos have demonstrated that the Fgf/Erk pathway both activates Gata6 transcription and represses Nanog's transcription (7,8,10-13). Finally, the model includes the observation that FGFR2 synthesis is upregulated by Gata6 (probably through an indirect mechanism) and downregulated by Nanog, as suggested by ChIP experiments (14,15). These regulations – which are schematically represented in Fig. 1 – constitute the GRN described in the model.

The differentiation status of a single cell is determined by the values of 4 intracellular variables: the first three variables represent the level of expression of a protein: Gata6 (G), Nanog (N) and FGFR2 (FR), whereas the fourth variable (ERK) represents the level of activity of the FGFR/Erk signaling pathway (comprised between 0 and 1). The temporal evolution of the 4 variables of the system is described by a set of

4 ordinary differential equations (S1)-(S4), which are identical to eqs (1)—(4) listed in the main text:

$$\frac{dG}{dt} = \left[vsg1 \frac{ERK^r}{Kag1^r + ERK^r} + vsg2 \frac{G^s}{Kag2^s + G^s} \right] \cdot \frac{Kig^q}{Kig^q + N^q} - kdg \cdot G \qquad \text{(S1)}$$

$$\frac{dN}{dt} = \left[vsn1 \frac{Kin1^u}{Kin1^u + ERK^u} + vsn2 \frac{N^v}{Kan^v + N^v} \right] \cdot \frac{Kin2^w}{Kin2^w + G^w} - kdn \cdot N \qquad \text{(S2)}$$

$$\frac{dFR}{dt} = vsfr1 \cdot \frac{Kifr}{Kifr + N} + vsfr2 \cdot \frac{G}{Kafr + G} - kdfr \cdot FR \qquad \text{(S3)}$$

$$\frac{dERK}{dt} = va \cdot FR \cdot \frac{Fp}{Kd + Fp} \cdot \frac{1 - ERK}{Ka + 1 - ERK} - vin \frac{ERK}{Ki + ERK} \qquad \text{(S4)}$$

The regulations affecting the synthesis of Gata6, Nanog and FGFR2 are described by Hill functions. In eq. (S1), the first term corresponds to the synthesis of Gata6 activated by the FGFR2-Erk pathway, the second one to the self-activation loop. The inhibitory influence of Nanog is assumed to affect both rates and thus appears as a multiplicative term. Synthesis of Nanog (eq. S2) is built in a similar way, taking into account that the ERK pathway has an inhibitory effect on Nanog synthesis. In eq. (S3), the first and second terms represent the synthesis of Fgf4 receptor that is inhibited by Nanog and activated by Gata6, respectively. The importance of the arrangement of terms –i.e. the logical architecture of the regulatory network– is discussed in a specific section of this Supporting information. The degradations of Gata6, Nanog and FGFR2 are described by the last terms of equations 1, 2 and 3, respectively. For simplicity, we assume that these reactions follow first order kinetics. In eq. (S4), the activation and inactivation of *ERK* are described by Michaelis-Menten equations. The activation of *ERK* increases linearly with the concentration of active FGFR2 and depends on the level of saturation of this receptor by extracellular Fgf4 (Fp). Parameter definitions and values are listed in Table S1. Parameter values were selected in order for the model to account for the available experimental data, in particular those presented in (7,8,16).

As illustrated in Fig. S4, depending on parameter values the model described by eqs (S1)-(S4) admits a single stable steady state (monostability), two stable steady states (bistability), or a coexistence between three stable steady states (tristability).

2. Two-cell system

To gain insight into the mechanism driving differentiation through Fgf4-modulation of the tristable system defined by eqs (S1-S4), we studied a model describing the intracellular GRN's of two neighboring cells and their interactions through the extracellular concentration of Fgf4, which now becomes a variable (*F*). The value of *F* is given by the average level of Fgf4 produced by both cells.

Experimental data obtained through the analysis of *Nanog*$^{-/-}$ embryos demonstrated a non-cell-autonomous role for Fgf4 in the maturation of the PrE (7,17). Indeed, Fgf4 – whose synthesis is stimulated by Nanog – is produced by Epi progenitors and reinforces PrE identity (7). The model includes this mechanism and assumes that Fgf4 synthesis is immediately followed by its secretion. In the model, every cell secretes Fgf4 at a rate that depends on its intracellular level of Nanog. Thus, the amount of Fgf4 synthetized by cells 1 and 2 are given by:

$$\frac{dFs_1}{dt} = vsf \cdot \frac{N_1^z}{Kaf^z + N_1^z} - kdf \cdot Fs_1 + vex \qquad \text{(S5)}$$

$$\frac{dFs_2}{dt} = vsf \cdot \frac{N_2^z}{Kaf^z + N_2^z} - kdf \cdot Fs_2 + vex \qquad \text{(S6)}$$

The Hill functions in eqs (S5) and (S6) describe the activation of Fgf4 synthesis by Nanog. The degradation of Fgf4 is assumed to follow first order kinetics. Parameter *vex* allows to simulate the addition of exogenous Fgf4, which occurs in some experimental protocols: in untreated embryos, *vex*=0. Parameter definitions and values are listed in Table S1. The extracellular concentration of Fgf4 (*F*) is defined as the average of *Fs1* and *Fs2*.

Experimental data suggest that local variability in Fgf4 concentration or availability is required for the emergence of both Epi and PrE progenitors within the ICM (12,13). In the model, this variability is introduced at the level of *Fp*, in the form of a deviation (γ) around the average extracellular concentration (*F*). In other words, the concentration of Fgf4 perceived by cell 1 (Fp_1) is slightly smaller than the average extracellular concentration (*F*), whereas cell 2 senses a concentration of FGF4 that is slightly higher than *F*:

$$Fp_1 = (1-\gamma) \cdot F \qquad \text{(S7)}$$

$$Fp_2 = (1+\gamma)\cdot F \qquad \text{(S8)}$$

with γ, a positive parameter that is always small (γ<<1). In the simulations of the 2-cell model, the value attributed to γ is 3%.

3. Cell population

Finally, we analyzed a model for a population of 25 cells arranged on a square 2-dimensional grid. The concentration of Fgf4 perceived by each cell corresponds to the average level of Fgf4 produced by the cell itself and by its 4 closest neighbors. This model also includes the effect of some noise on the spatial distribution of the Fgf4 molecules in the extracellular space, in the form of a deviation (γ_i) around its average concentration. Thus, the concentration of Fgf4 perceived by a cell *i* (Fp_i) is given by:

$$Fp_i = \frac{(1+\gamma_i)}{5}\left(Fs_i + \sum_{j=1}^{4} Fs_{i,j}\right) \qquad \text{(S9)}$$

where summation is made on the four nearest neighbors of cell *i*, and where γ_i is a number attributed to cell *i* at the beginning of each simulation. Results are similar when the summation is made on the eight nearest neighbors of cell *i*. The value of γ_i is taken randomly from a uniform distribution in the [-γ, γ] interval and remains the same for the whole simulation time. The default value for γ is 0.1. Each *Fsi* is computed as in the 2-cell model (eqs S5 or S6).

Logical architecture of the regulatory network

In this section, we focus on the system describing the interactions between the transcription factors Nanog and Gata6 and their interplay with the Fgf/Erk signaling pathway within one cell (eqs(S1)-(S2)). We analyze the consequences of the precise arrangement of terms in these equations. How auto-activation, cross-inhibition and Erk signaling combine does not only determine the possible existence of tristability but also governs the dynamical behavior or the model. We thus reasoned about the adequacy between this arrangement and key experimental observations about Epi and PrE cell specification. We considered the eight logical structures possible for this network. The results of this investigation are summarized in Table 1 (see main text), where successive

rows depict the different logical architectures and their suitability to describe experimental observations. In all cases, we assume that this arrangement is of the same type for the evolution equations of Nanog and Gata6.

We first examined if the logical structure is compatible with observations on mutant embryos treated with Fgf4 or with Fgf/Erk inhibitors. Mutant embryos indeed display two phases of sensitivity to Fgf/Erk signaling. In Nanog$^{-/-}$ embryos, which do not express Nanog, Gata6 does not increase if the embryo is treated early with Fgf/Erk inhibitors (phase I). However, if Fgf/Erk inhibitors are applied later, when Gata6 has already increased to some intermediate level, Gata6 is still able to increase (phase II), indicating that Erk signaling has become dispensable (7). Similarly, in Gata6$^{-/-}$ embryos treated with Fgf4, early treatment prevents the increase in Nanog, while in response to later treatment, all cells adopt an Epi fate (8; see also Fig. 6 in the main text). If the logical structure is compatible with these observations, we next examine the possible existence of tristability in the full model (eqs(S1)-(S4))

When two terms in the equations are multiplied, and are therefore closely linked because the presence of each term is required to produce an effect, they correspond to the logical command "AND", while they correspond to the command "OR" when they are added, given that each term can produce a partial effect on its own. The combination retained in eqs (S1)-(S2) is thus: CI.AND.[AA.OR.ERK]. As explained in the main text, this logical architecture yields good agreement with experimental observations. We now describe why this is not the case for the alternative logical architectures.

• ERK.AND.[AA.OR.CI]

This logical structure corresponds to the following equation for G:

$$\frac{dG}{dt} = \frac{ERK^r}{Kag1^r + ERK^r}\left[vsg1\frac{G^s}{Kag2^s + G^s} + vsg2\frac{Kig^q}{Kig^q + N^q}\right] - kdg \cdot G \qquad \text{(S10)}$$

The model then predicts that when N~0 (Nanog$^{-/-}$ mutant), Gata6 cannot remain high when ERK=0 (i.e., in presence of Fgf/Erk inhibitors), which is in contrast with the experimental observations that show that Gata6 can remain high if Fgf/Erk inhibitors are added after Gata6 has reached a sufficient level (phase II).

• AA.AND.[CI.OR.ERK]

This logical structure corresponds to the following equations for N and G:

$$\frac{dN}{dt} = \frac{N^v}{Kan^v + N^v}\left[vsn2\frac{Kin2^w}{Kin2^w + G^w} + vsn1\frac{Kin1^u}{Kin1^u + ERK^u}\right] - kdn \cdot N \qquad \text{(S11)}$$

$$\frac{dG}{dt} = \frac{G^s}{Kag2^s + G^s}\left[vsg2\frac{Kig^q}{Kig^q + G^q} + vsg1\frac{ERK^r}{Kag1^r + ERK^r}\right] - kdg \cdot G \qquad \text{(S12)}$$

In this system, the steady state N=G=0 is always stable and will not allow the initial increase of Nanog and Gata6, especially in view of the fact that the basin of attraction of the trivial steady state is rather large (see Fig. S1).

• ERK.OR.[AA.AND.CI]

This logical structure corresponds to the following equations for N and G:

$$\frac{dN}{dt} = vsn1\frac{Kin1^u}{Kin1^u + ERK^u} + \left[vsn2\frac{N^v}{Kan^v + N^v} \cdot \frac{Kin2^w}{Kin2^w + G^w}\right] - kdn \cdot N \qquad \text{(S13)}$$

$$\frac{dG}{dt} = vsg1\frac{ERK^r}{Kag1^r + ERK^r} + \left[vsg2\frac{G^s}{Kag^s + G^s} \cdot \frac{Kig^q}{Kig^q + N^q}\right] - kdg \cdot G \qquad \text{(S14)}$$

This system of equations does not exhibit tristability for the explored range of parameter values. This is in agreement with the view proposed in the main text that tristability arises when a transcription factor increases either because its own level is high or because the level of the other one is low. Multiplication of cross-inhibition and auto-activation does not correspond to such a situation, and incorporation of the ERK signaling pathway does not allow recovery of the interactions required for tristability.

• CI.OR.[AA.AND.ERK]

This logical structure corresponds to the following equation for N:

$$\frac{dN}{dt} = vsn1\frac{Kin2^w}{Kin2^w + G^w} + \left[vsn2\frac{N^v}{Kan^v + N^v} \cdot \frac{Kin1^u}{Kin1^u + Erk^u}\right] - kdn \cdot N \qquad \text{(S15)}$$

Then, when G~0 (Gata6$^{-/-}$ mutant), Nanog can increase when ERK is high (high level of Fgf4). This prediction does not hold with the observation that no increase in Nanog occurs during phase I. Symmetrically, the evolution equation for G is not compatible with observations on Nanog$^{-/-}$ mutants during phase I.

• AA.OR.[CI.AND.ERK]

This logical structure corresponds to the following equations for N and G:

$$\frac{dN}{dt} = vsn1\frac{N^v}{Kan^v + N^v} + \left[vsn2\frac{Kin2^w}{Kin2^w + G^w} \cdot \frac{Kin1^u}{Kin1^u + ERK^u} \right] - kdn \cdot N \qquad \text{(S16)}$$

$$\frac{dG}{dt} = vsg2\frac{G^s}{Kag2^s + G^s} + \left[vsg1\frac{Kig^q}{Kig^q + N^q} \cdot \frac{ERK^r}{Kag1^r + ERK^r} \right] - kdg \cdot G \qquad \text{(S17)}$$

These evolution equations are compatible with the observations on mutant embryos. The system also displays tristability, as shown in Fig. S2. However, in this case, the intermediate state corresponding to the ICM is stable on the whole range of Fgf4 concentrations, because auto-activation and cross-inhibition are not mutually exclusive. This bifurcation diagram cannot account for experimental observations showing that Fgf/Erk inhibitors induce all ICM cells to specify into Epi cells, while high Fgf4 induce all cells to specify into PrE cells (7,16).

• **AA.OR.CI.OR.ERK**

This logical structure corresponds to the following equation for N:

$$\frac{dN}{dt} = vsn1\frac{N^v}{Kan^v + N^v} + vsn2\frac{Kin2^w}{Kin2^w + G^w} + vsn3\frac{Kin1^u}{Kin1^u + ERK^u} - kdn \cdot N \quad \text{(S18)}$$

When G∼0 (Gata6$^{-/-}$ mutant), Nanog can increase when ERK is high (high level of Fgf4), while no increase in Nanog is observed experimentally during phase I. Symmetrically, the evolution equation for G is not compatible with observations on Nanog$^{-/-}$ mutants during phase I.

• **AA.AND.CI.AND.ERK**

This logical structure corresponds to the following equation for N:

$$\frac{dN}{dt} = vsn1\frac{N^v}{Kan^v + N^v} \cdot \frac{Kin2^w}{Kin2^w + G^w} \cdot \frac{Kin1^u}{Kin1^u + ERK^u} - kdg \cdot N \qquad \text{(S19)}$$

When G∼0 (Gata6$^{-/-}$ mutant), Nanog cannot remain high when ERK is high (high Fgf4), which is in contradiction with the experimental observations showing that Nanog can remain high when Fgf4 is administered when Nanog has reached a sufficient level (phase II). Symmetrically, the evolution equation for G is not compatible with observations on Nanog$^{-/-}$ mutants during phase II.

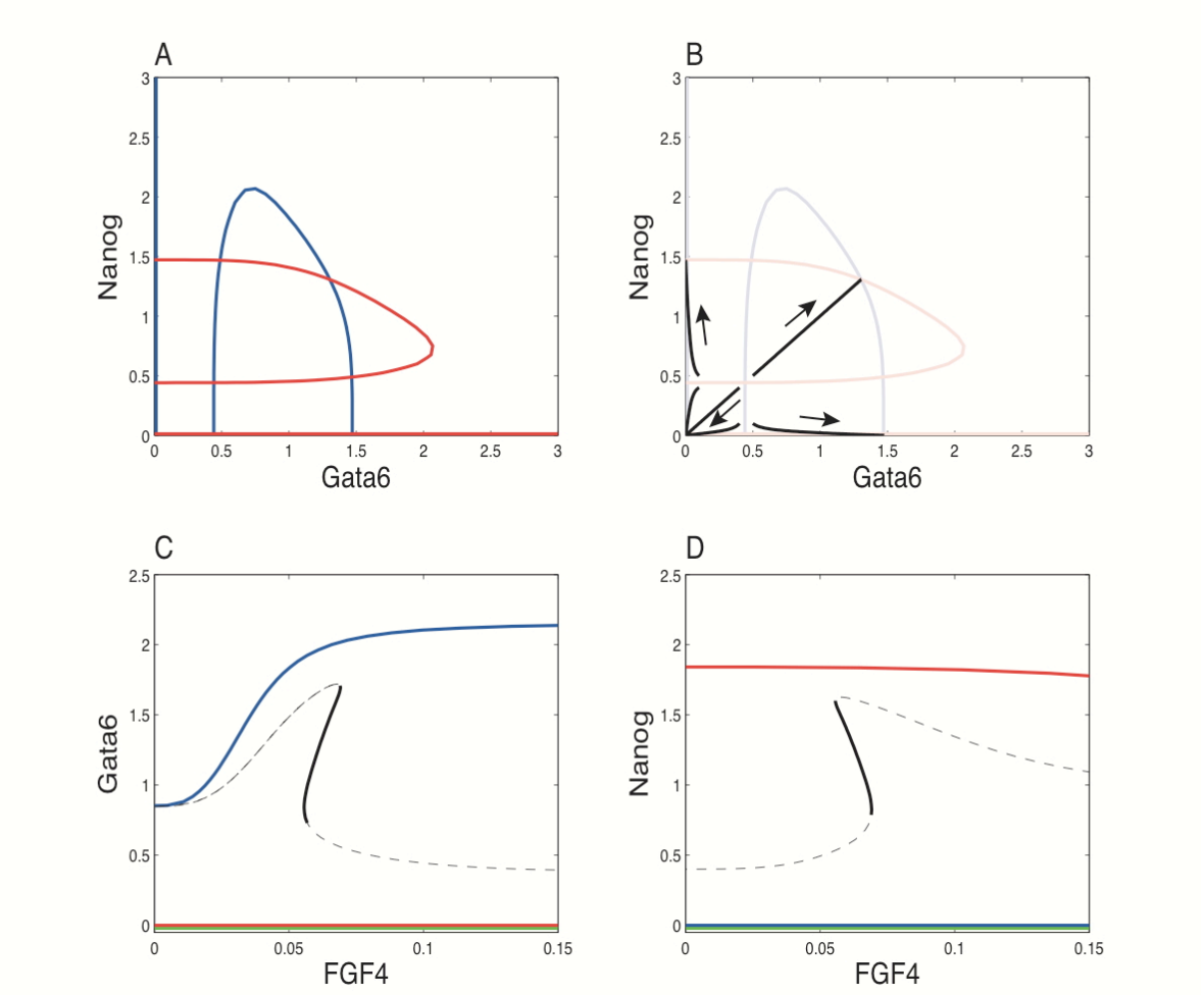

Fig. S1 Phase space portrait and bifurcation diagram of a modified version of the model corresponding to the AA.AND.[CI.OR.ERK] logical structure. (A, B) Phase portrait showing the nullclines of the 2-variable (N, G) system defined by eqs (S11)-(S12) (red for the N nullcline and blue for the G nullcline). In (B), black lines show examples of trajectories directed towards the four possible (stable) steady states, one of which corresponds to the (0, 0) state. (C, D) Bifurcation diagrams showing the steady state of Gata6 and Nanog as a function of FGF4 concentration. The bifurcation diagram is established using AUTO, for the full system defined by eqs (S11), (S12), (S3) and (S4). The steady state N=G=0 is always stable and will not allow any initial increase of Nanog and Gata6, given that the basin of attraction of the trivial steady state is rather large, as shown in (B). Parameter values are given in Table S1.

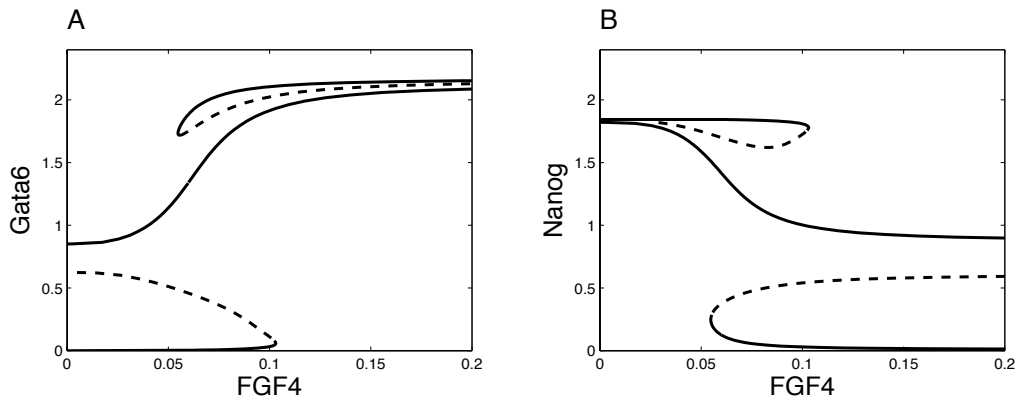

<u>Fig. S2</u> Bifurcation diagram for a modified version of the model corresponding to the AA.OR.[CI.AND.ERK] logical structure. The diagram is established using AUTO, for eqs (S16), (S17), (S3) and (S4). Parameter values are given in Table S1. This version of the model also displays tristability but, in this case, the intermediate state corresponding to the ICM is stable on the whole range of Fgf4 concentrations. These bifurcation diagrams cannot account for experimental observations showing that Fgf/Erk inhibitors induce all ICM cells to specify into Epi cells, while high Fgf4 induce all cells to specify into PrE cells (7,16).

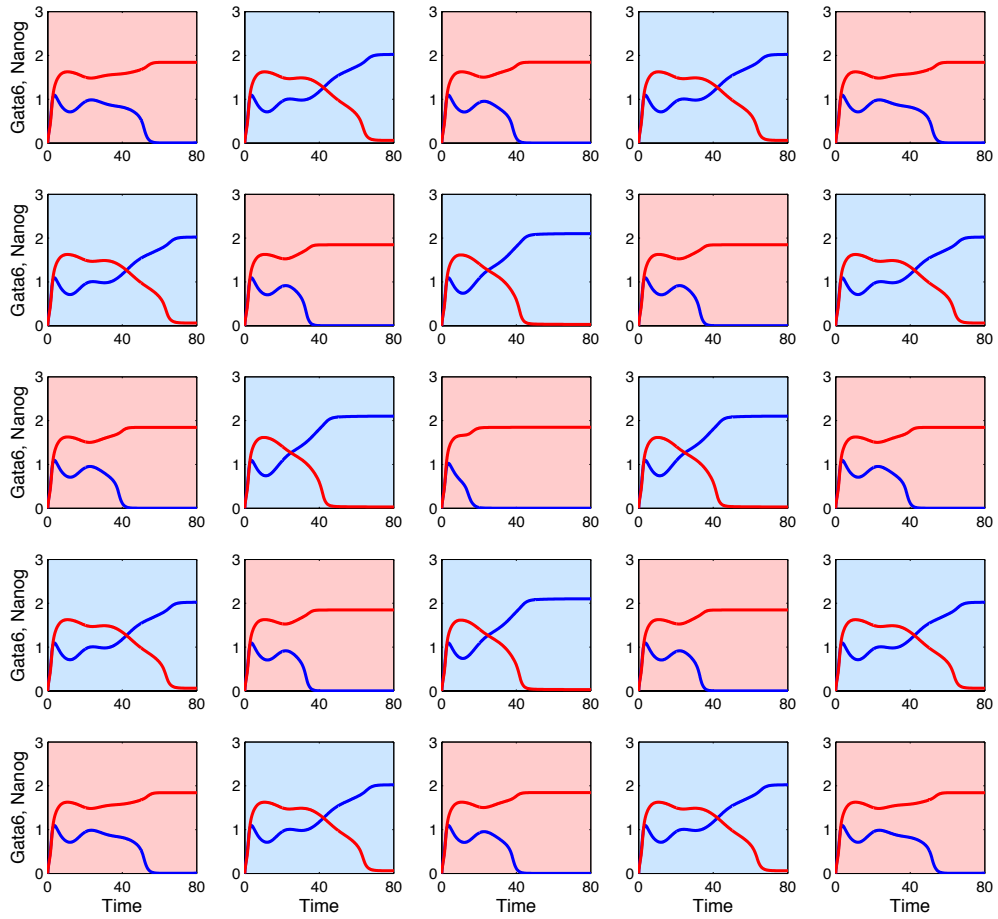

Fig. S3 Salt-and-pepper pattern originating from a single heterogeneity. Specification into Epi and PrE cells in a population of 25 initially identical cells where only the central cell has a lower value for γ_i (-0.1), while γ_i =0 for other cells. Because it perceives less Fgf4, the central cell evolves towards an Epi fate, characterized by high Nanog levels (red curve). Thus, it will secrete more Fgf4, which will be perceived by its neighbors that will thus evolve towards the PrE fate, characterized by high Gata6 levels (blue curve). Because these cells secrete less Fgf4, their own neighbors will in turn tend towards the Epi fate, etc. Such a network of interactions through extracellular Fgf4 will induce a mosaic pattern in the simulated 5x5 configuration of cells. Except for the γ_i's, parameter values and initial conditions are the same as in Fig. 4.

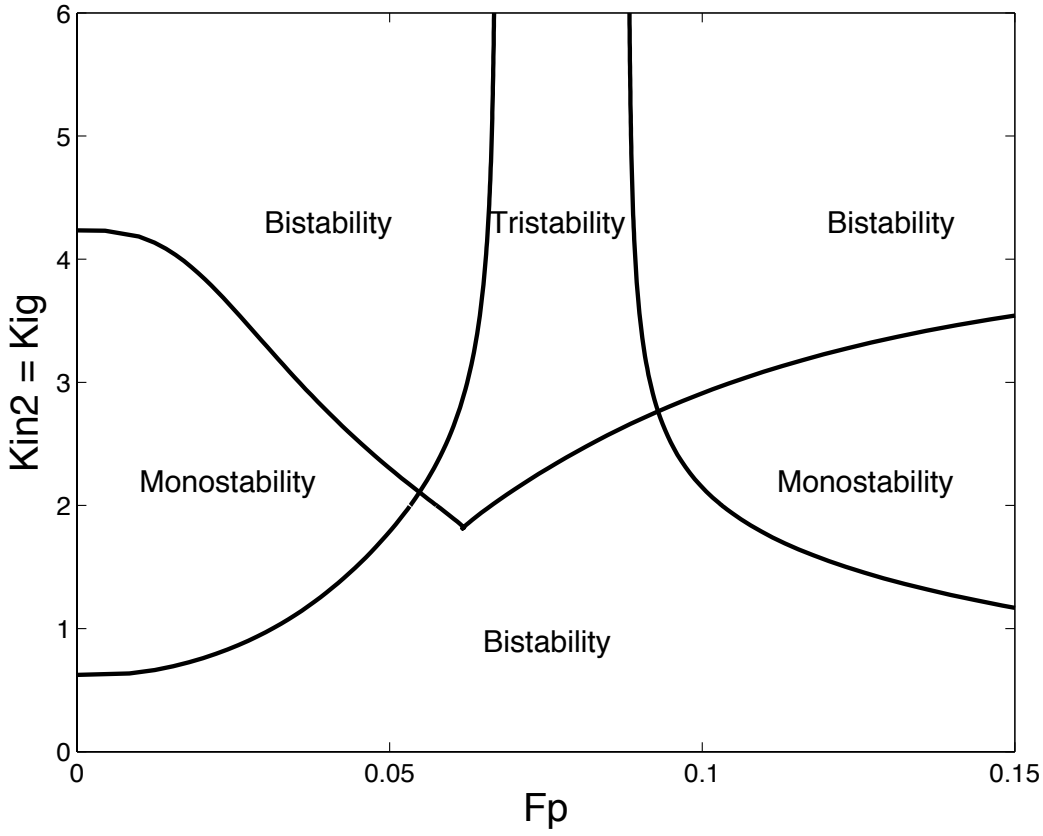

Fig. S4 Two-parameter bifurcation diagram of the model. The diagram is established for eqs (1)-(4) using AUTO, as a function of the extracellular level of FGF4 (*Fp*) and the cross-inhibition constants *Kin2*=*Kig*. Other parameter values are listed in Table S1.

Symbol	Definition	Value
vsg1	Maximum rate of Gata6 synthesis caused by ERK activation	1.202
vsg2	Maximum rate of Gata6 synthesis caused by its auto-activation	1
vsn1	Basal rate of Nanog synthesis	0.856
vsn2	Maximum rate of Nanog synthesis caused by its auto-activation	1
vsfr1	Basal rate of FGFR2 synthesis	2.8
vsfr2	Maximum rate of FGFR2 synthesis caused by Gata6 activation	2.8
vex	Basal rate of Fgf4 synthesis	0
vsf	Maximum rate of Fgf4 synthesis caused by Nanog activation	0.6
va	ERK activation rate	20
vi	ERK inactivation rate	3.3
kdg	Gata6 degradation rate	1
kdn	Nanog degradation rate	1
kdfr	FGFR2 degradation rate	1
kdf	Fgf4 degradation rate	0.09
Kag1	Threshold constant for the activation of Gata6 synthesis by ERK	0.28
Kag2	Threshold constant for Gata6 auto-activation	0.55
Kan	Threshold constant for Nanog auto-activation	0.55
Kafr	Threshold constant for the activation of FGFR2 synthesis by Gata6	0.5
Kaf	Threshold constant for the activation of Fgf4 synthesis by Nanog	5
Kig	Threshold constant for the inhibition of Gata6 synthesis by Nanog	2
Kin1	Threshold constant for the inhibition of Nanog synthesis by ERK	0.28
Kin2	Threshold constant for the inhibition of Nanog synthesis by Gata6	2
Kifr	Threshold constant for the inhibition of FGFR2 synthesis by Nanog	0.5
Ka	Michaelis constant for activation of the ERK pathway	0.7
Ki	Michaelis constant for inactivation of the ERK pathway	0.7
Kd	Michaelis constant for activation of the ERK pathway by Fgf4	2
r	Hill coefficient for the activation of Gata6 synthesis by ERK	3
s	Hill coefficient for Gata6 auto- activation	4
q	Hill coefficient for the inhibition of Gata6 synthesis by Nanog	4
u	Hill coefficient for the inhibition of Nanog synthesis by ERK	3
v	Hill coefficient for Nanog auto-activation	4
w	Hill coefficient for the inhibition of Nanog synthesis by Gata6	4
z	Hill coefficient for the activation of Fgf4 synthesis by Nanog	4

Table S1 Values of the parameters used in the simulations of equations (1)-(4) unless specified. These values are taken from Bessonnard *et al*. (8), except for *kdf,* which was slightly modified to illustrate the effect of this parameter on the Epi/PrE cells ratio.

Symbol	Definition	Value
vsg1	Maximum rate of Gata6 synthesis caused by ERK activation	0.78
vsn1	Basal rate of Nanog synthesis	1.393
va	ERK activation rate	40.46
Kag2	Threshold constant for Gata6 auto-activation	1
Kan	Threshold constant for Nanog auto-activation	1
Kig	Threshold constant for the inhibition of Gata6 synthesis by Nanog	1
Kin2	Threshold constant for the inhibition of Nanog synthesis by Gata6	1
r	Hill coefficient for the activation of Gata6 synthesis by ERK	1
u	Hill coefficient for the inhibition of Nanog synthesis by ERK	1

Table S2 Example of another set of parameter values giving rise to tristability corresponding to the 3 physiological states: ICM, Epi and PrE. The values of the parameters not mentioned in this table are similar to those listed in Table S1.

Reaction step	Reaction	Propensity
1	Gata6 synthesis	$\left[vsg1' \frac{ERK^r}{Kag1'^r + ERK^r} + vsg2' \frac{G^s}{Kag2'^s + G^s} \right] \cdot \frac{Kig'^q}{Kig'^q + N^q}$
2	Gata6 degradation	$kdg \cdot G$
3	Nanog synthesis	$\left[vsn1' \frac{Kin1'^u}{Kin1'^u + ERK^u} + vsn2' \frac{N^v}{Kan'^v + N^v} \right] \cdot \frac{Kin2'^w}{Kin2'^w + G^w}$
4	Nanog degradation	$kdn \cdot N$
5	FGFR2 synthesis	$vsfr1' \cdot \frac{Kifr'}{Kifr' + N} + vsfr2' \cdot \frac{G}{Kafr' + G}$
6	FGFR2 degradation	$kdfr \cdot FR$
7	Erk activation	$va \cdot FR \cdot \frac{Fp}{Kd' + Fp} \cdot \frac{ERKtot - ERK}{Ka' + ERKtot - ERK}$
8	Erk inactivation	$vin' \frac{ERK}{Kin' + ERK}$
9	FGF4 production	$vsf' \frac{N^z}{Kaf'^z + N^z}$
10	FGF4 degradation	$kdf.Fs$

Table S3 Reaction steps and corresponding propensities considered in the stochastic version of the model based on Gillespie's algorithm (18). Parameter values are given in Table 1, except that parameters noted with a prime are multiplied by Ω.

Supporting references

1. Molkentin JD, Antos C, Mercer B, Taigen T, Miano JM, et al. 2000. Direct activation of a GATA6 cardiac enhancer by Nkx2.5: evidence for a reinforcing regulatory network of Nkx2.5 and GATA transcription factors in the developing heart. Dev Biol 217: 301-309.
2. Fujikura J, Yamato E, Yonemura S, Hosoda K, Masui S, et al. 2002. Differentiation of embryonic stem cells is induced by GATA factors. Genes Dev 16: 784-789.
3. Boyer LA, Lee TI, Cole MF, Johnstone SE, Levine SS, et al. 2005. Core transcriptional regulatory circuitry in human embryonic stem cells. Cell 122: 947-956.
4. Shimosato D, Shiki M, Niwa H. 2007. Extra-embryonic endoderm cells derived from ES cells induced by GATA factors acquire the character of XEN cells. BMC Dev Biol 7: 80.
5. Singh AM, Hamazaki T, Hankowski KE, Terada N. 2007. A heterogeneous expression pattern for Nanog in embryonic stem cells. Stem cells 25: 2534-2542.
6. Kim J, Chu J, Shen X, Wang J, Orkin SH. 2008. An extended transcriptional network for pluripotency of embryonic stem cells. Cell 132: 1049-1061.
7. Frankenberg S, Gerbe F, Bessonnard S, Belville C, Pouchin P, et al. 2011. Primitive Endoderm Differentiates via a Three-Step Mechanism Involving Nanog and RTK Signaling. Dev Cell 21: 1005-1013.
8. Bessonnard S., De Mot L., Gonze D., Barriol M., Dennis C., Goldbeter A., Dupont G. and Chazaud C. 2014. Gata6, Nanog and Erk signaling control cell fate in the inner cell mass through a tristable regulatory network. Development 141: 3637-3648.
9. Fidalgo M, Faiola F, Pereira CF, Ding J, Saunders A, et al. 2012. Zfp281 mediates Nanog autorepression through recruitment of the NuRD complex and inhibits somatic cell reprogramming. Proc Nat Acad Sci USA 109: 16202-16207.
10. Hamazaki T, Kehoe SM, Nakano T, Terada N. 2006. The Grb2/Mek pathway represses Nanog in murine embryonic stem cells. Mol Cell Biol 26: 7539-7549.
11. Santostefano KE, Hamazaki T, Pardo CE, Kladde MP, Terada N. 2012. Fibroblast growth factor receptor 2 homodimerization rapidly reduces transcription of the pluripotency gene Nanog without dissociation of activating transcription factors. J. Biol. Chem. 287: 30507-30517.
12. Kang M, Piliszek A, Artus J, Hadjantonakis AK. 2013. FGF4 is required for lineage restriction and salt-and-pepper distribution of primitive endoderm factors but not their initial expression in the mouse. Development 140: 267-279.

13. Krawchuk D, Honma-Yamanaka N, Anani S, Yamanaka Y. 2013. FGF4 is a limiting factor controlling the proportions of primitive endoderm and epiblast in the ICM of the mouse blastocyst. Dev. Biol. 384: 65-71.
14. Niakan KK, Ji H, Maehr R, Vokes SA, Rodolfa KT, et al. 2010. Sox17 promotes differentiation in mouse embryonic stem cells by directly regulating extraembryonic gene expression and indirectly antagonizing self-renewal. Genes Dev 24: 312-326.
15. Ma Z, Swigut T, Valouev A, Rada-Iglesias A, Wysocka J. 2011. Sequence-specific regulator Prdm14 safeguards mouse ESCs from entering extraembryonic endoderm fates. Nature Struct & Mol Biol 18: 120-127.
16. Yamanaka Y, Lanner F, Rossant J. 2010. FGF signal-dependent segregation of primitive endoderm and epiblast in the mouse blastocyst. Development 137: 715-724.
17. Messerschmidt DM, Kemler R. 2010. Nanog is required for primitive endoderm formation through a non-cell autonomous mechanism. Dev Biol 344: 129-137.
18. Gillespie D. 1976. A general method for numerically simulating the stochastic time evolution of coupled chemical reaction. J. Comput. Phys. 22: 403-434.